Black Start Service from Offshore Wind Power Plant using IBESS

Chaudhary, Sanjay K.; Teodorescu, Remus; Svensson, Jan R.; Kocewiak, Lukasz; Johnson, Philip; Berggren, Bertil

Published in:
2021 IEEE Madrid PowerTech, PowerTech 2021 - Conference Proceedings

DOI (link to publication from Publisher):
10.1109/PowerTech46648.2021.9494851

Publication date:
2021

Document Version
Accepted author manuscript, peer reviewed version

Citation for published version (APA):
Chaudhary, S. K., Teodorescu, R., Svensson, J. R., Kocewiak, L., Johnson, P., & Berggren, B. (2021). Black Start Service from Offshore Wind Power Plant using IBESS. In *2021 IEEE Madrid PowerTech, PowerTech 2021 - Conference Proceedings* (pp. 1-6). Article 9494851 IEEE (Institute of Electrical and Electronics Engineers). https://doi.org/10.1109/PowerTech46648.2021.9494851

Black Start Service from Offshore Wind Power Plant using IBESS

Sanjay K. Chaudhary
Dept. of Energy Technology
Aalborg University
Aalborg, Denmark
skc@et.aau.dk

Remus Teodorescu
Dept. of Energy Technology
Aalborg University
Aalborg, Denmark
ret@et.aau.dk

Jan R. Svensson
Power Grids Research
Hitachi ABB Power Grids
Västerås, Sweden
jan.r.svensson@hitachi-powergrids.com

Łukasz H. Kocewiak
Electrical System Design & Grid Integration
Ørsted Offshore
Gentofte, Denmark
lukko@orsted.dk

Philip Johnson
Grid Connections, New Markets
Ørsted Offshore
London, U.K.
phijo@orsted.co.uk

Bertil Berggren
Power Grids Research
Hitachi ABB Power Grids
Västerås, Sweden
bertil.berggren@hitachi-powergrids.com

***Abstract*—The share of renewables in the power system is increasing rapidly. Large offshore wind power plants (OWPPs) are developed at a high pace and conventional fossil fuel-based plants are decommissioned. Consequently, there will be a risk of insufficient amount of power plants providing black start functionality for system restoration after a black out. This paper proposes a STATCOM with a battery energy storage that is located at the point of common connection to an OWPP that together can provide a reliable black start services to the power grid. The concept is demonstrated by using time domain simulations in PSCAD. The STATCOM functionality provides fast and dynamic reactive power management and the battery unit provides active power balancing capability to maintain the frequency within a tolerable range specified by the system operator. The simulation results fulfill the success criteria for the black start and confirm its feasibility for practical implementation.**

Keywords—battery storage, black start, frequency control, grid forming converter, offshore wind power plant, power system restoration, STATCOM, voltage control.

I. Introduction

A number of large offshore wind power plants (OWPPs) have been developed especially in Europe and many more are under development worldwide in order to reduce the emission of greenhouse gases [1]. Wind is a meteorological phenomenon resulting in varying wind power all the time. Therefore, wind power inherently has a non-dispatchable nature. The power changes with the wind speed and is zero when the wind speed is below the cut-in speed. With more renewables, the share of conventional fossil fuel-based plants is decreasing rapidly. Consequently, there is a potential risk of missing reliable sources which can provide the black start service for power system restoration.

According to PJM Manual 36 for system restoration [2] a black start unit must be capable of starting itself from shutdown condition and start delivering power to the grid without any assistance from the system. Likewise, National Grid specifies the following requirements for the black start functionality [3]:

- Ability to start up itself independent of external supplies;
- Ability to energize a part of the network with purely reactive power exchange;
- Ability to accept block load demand.

An overview of requirements for black start provision is given in [4]. Thus, non-dispatchable sources like wind and other renewable energy sources would not qualify by themselves for the black-start service.

A large STATCOM integrated with a battery storage, referred to as IBESS, was initially proposed in [5],[6] to enable the black start capability of an OWPP. The IBESS is located at point of common coupling. The STATCOM functionality provides fast and dynamic reactive power management and hence contributes to the voltage regulation. Likewise, the battery storage enables the bidirectional exchange of active power with the system and thus, the IBESS can provide inertial and frequency regulation services [7].

As stipulated by PJM and National Grid, an IBESS enables an OWPP to energize itself from shut-down condition and operate in an islanded mode with stable frequency and voltage profile [8]. With the help of IBESS, the OWPP can meet its auxiliary power demand and keep itself running even in no wind conditions. Thus, the OWPP can remain in standby mode to quickly provide the black-start service. Provided that the IBESS has enough stored energy, the OWPP can provide black start service by energizing a part of the onshore grid and accepting block load connection. At present black start service from an OWPP with the help of IBESS is a novel concept, which is proposed in this paper. A detailed OWPP and onshore grid model is developed together with an adapted IBESS and OWPP controller. Time domain simulations are performed to display the fulfilment of the success criteria for black start.

The paper is organized as follows. The test network for this study is described in Section II. The IBESS topology and its grid forming controller has been described in Section III. Section IV presents the simulation results for the sequence of events necessary for the restoration of a part of the onshore grid by the IBESS and the OWPP. The results are finally concluded in Section V.

II. Test OWPP Model

A. OWPP Network

The test OWPP model is based on the 1386 Hornsea Two OWPP [9]. A third of the plant has been modelled here as shown in Fig. 1. The offshore grid model comprises of the

The project was financed by Innovation Fund Denmark with grant number 8055-00074B.

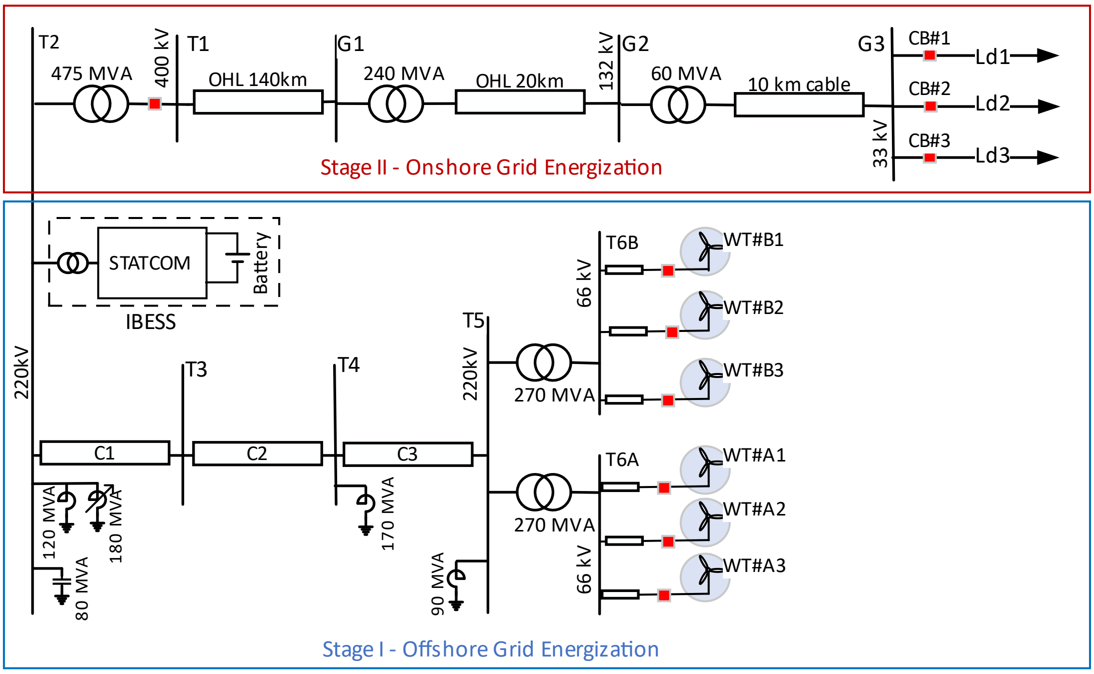

Fig. 1. Schematic diagram of test OWPP network along with the onshore grid and 3x20 MW block loads.

220 kV export cable, associated shunt filters and reactors, and 2x270 MVA, 220/66 kV transformers at the collector bus. The high voltage (HV) export cable comprise of 40 km underground cable (C1) in flat layout, and two sections of submarine cables (C2 and C3) each 60 km long with 90 Mvar of shunt reactors (Q4) in the middle at the bus T4. The submarine cables have a trefoil layout inside a pipe. In addition, (120 – 300) Mvar variable shunt reactor at the bus T2 and 170 Mvar reactor at the bus T4 are provided for reactive power compensation. There is 80 Mvar capacitive shunt filter connected at the bus T2. All these components are assumed to be connected in this study.

In order to retain the transient response characteristics, the HV export cables are modelled using their geometrical core and layout details and phase dependent travelling wave model is derived. Similarly, the magnetic saturation characteristics of the transformer core is included in the model.

The nominal ratings and the selected base values for the IBESS and the WT are given in Table I. While the OWPP has 55 WT units, here only 37 units have been considered. These 37 units are aggregated into 6 groups, comprising of 4, 5, 6, or 9 units. The ratings of the WT group equivalent are accordingly scaled up. The 66 kV collector feeders are represented by a series combination of 0.68 Ω resistor, 5.2 mH inductor and 5.1 µF shunt capacitor on the turbine side.

B. WT Model

The WTs are modelled in terms of the average model of the grid-side converters along with their converters. An ideal dc link is assumed that implies sufficient wind power is available at all instants. The grid following control tracks the active and reactive power references together with the ac voltage magnitude regulation. The controller is implemented in the synchronously rotating *dq*-coordinate frame. In this study, the WT is in the voltage regulation mode, which is realized by injecting the reactive current in proportion to the

TABLE I. NOMINAL RATINGS OF IBESS, 8 MW WT UNIT.

Base values	Unit	IBESS	8 MW WT unit
Active power (P)	MW	50	8
Reactive power (Q)	Mvar	100	
Power factor		-	0.9
Nominal MVA (Base)	MVA	111.8	8.889
Nominal rms voltage	kV (l-l)	33	0.69
Base voltage (peak)	kV (l-g)	26.94	0.5634
Nominal rms current	kA	1.956	7.4377
Base current (peak)	kA	2.766	10.518
Base impedance	Ω	9.740	0.05356
Base frequency	Hz	50	50

voltage deviation from the nominal value. A droop frequency regulation of 5% in the steady state is implemented.

C. Part of Onshore Grid for Energization

A 475 MVA, 400/220 kV transformer is connected between the OWPP and a 140 km long overhead line (OHL), shown in Fig 1. With 9.88 S susceptance, the line would generate 86.49 Mvar reactive power at 1.0 pu voltage. Moreover, as an extreme case, no shunt reactors were connected to the line. These considerations are made in order to emulate the proposed requirement of 100 Mvar leading reactive power supply capability of the black start unit [10]. Further down it is connected to a 20 km long line at 132 kV and finally to the block loads at 33 kV through a 10 km long cable. There are three block loads of 20 MW size each at the remote end. The loads are modelled as constant resistances of 54.45 Ω.

D. Transformer Saturation

Magnetizing characteristics of the transformer and its saturation play a critical role during the switching transients. The magnetizing current can be large and highly non-linear and depends on the point of switching and residual magnetic field at the instant. In this work, the magnetic hysteresis loop is ignored, and the transformer magnetic saturation is modelled in terms of airgap reactance, which is

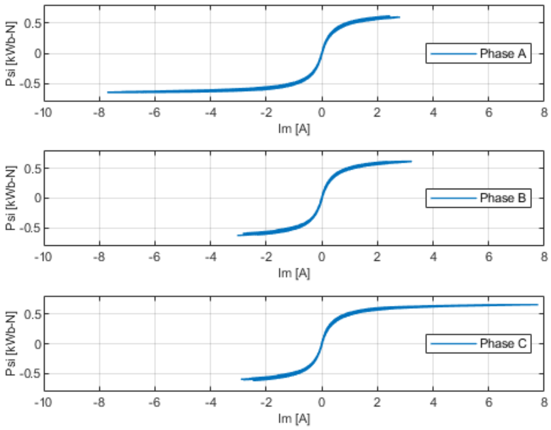

Fig. 2. Transformer magnetizing characteristic of IBESS transformer.

assumed to be the double of the leakage reactance, and the knee point voltage, assumed to be 1.17 pu. The resultant magnetic flux-linkage vs. magnetizing current characteristic of the IBESS transformer is displayed in Fig. 2. It shows a highly asymmetric peak current in phases A and C due to the saturation of the flux during the switching of the OHL. Under steady state conditions, this curve is symmetric about both the flux-linkage and the current axes. The saturation characteristics had a small effect in the previous work reported in [8] as soft-charging was used and the WT unit transformers were located far from IBESS.

III. IBESS Topology and its Control

Modular multilevel converter (MMC) is the preferred topology for high voltage and high power STATCOM applications. For the IBESS, a 20 kVdc battery unit is integrated with the STATCOM, which is connected to the 33 kVac bus. Since the dc voltage is too low for the MMC using the double star half-bridge (DSHB) topology, the double star full bridge MMC with centralized energy storage (DSFB-CES) has been selected [11].

A single-line diagram of the IBESS and its controllers are shown in Fig. 3. All the control parameters are defined in Table II. The grid forming controller of the IBESS has two parts – (i) power synchronization control (PSC) and (ii) the voltage magnitude controller (VMC).

A. Power synchronization Control

The PSC, proposed in [12] emulates the swing equation of the synchronous machines. The tuning of the controller for grid connected application is described in [13]. From the block diagram in Fig 3(b), the IBESS frequency deviation, $\Delta\omega$, corresponds to the deviation in IBESS power, ΔP, and is given by,

$$\Delta\omega(s) = \frac{1}{2Hs+\frac{k_d s}{s+\omega_d}+k_g}\Delta P(s). \tag{1}$$

Here, the parameter, H, indicates the inertia constant as defined in the conventional power system. It tends to resist the frequency deviations. The damping parameter k_d tends to damp out the high frequency oscillations if any in the power deviation. In steady state, as (1) can be written as,

$$\Delta P = k_g \Delta\omega. \tag{2}$$

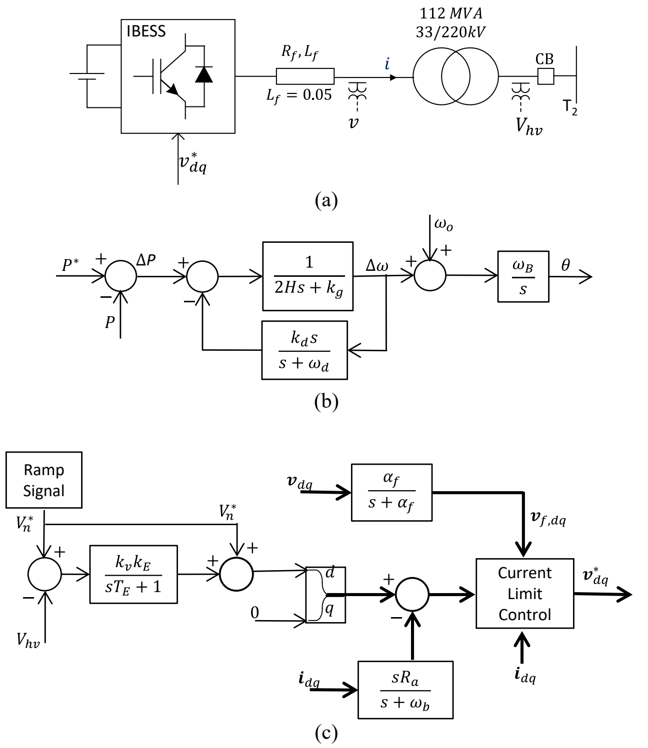

Fig. 3. (a) Schematic diagram of the IBESS. (b) Power synchronization control (PSC). (c) Voltage magnitude control (VMC).

TABLE II. Parameters of IBESS Controller.

Parameter	Symbol	Value
Parameter k_g	k_g	62.5 pu
Base frequency	ω_B	100π rad/s
Mechanical inertia constant	H	5 s
Damping controller gain	k_d	62.5 pu
Damping controller bandwidth	ω_d	16 rad/s
Voltage regulation gain	$k_v k_E$	1.25 pu
Voltage regulator time constant	T_E	0.05 s
Active damping resistance	R_a	0.05 pu
Cut-off frequency	ω_b	0.2 rad/s
Current magnitude limit	$\lvert I_{max}\rvert$	1.1 pu
Equivalent inductance	L_f	0.05 pu
Current control bandwidth	α	5000 rad/s
Current control gain	αL_f	0.7958 pu
Voltage filter bandwidth	α_f	2500 rad/s
Voltage magnitude limit	$\lvert V_{max}\rvert$	1.1 pu

Thus, the reciprocal of the parameter, k_g, indicates the droop frequency response of the IBESS. In this study, 1.6% frequency regulation droop has been considered by setting $k_g = 62.5$ pu. The PSC determines the frequency and phase angle, θ, of the IBESS in grid forming control mode. The angle θ is used in all the Park's transformations and inverse transformations.

B. Voltage Magnitude Control

The VMC determines the magnitude of the voltage to be generated by the IBESS. The VMC comprises of the nominal voltage reference, V^*_n. It is augmented by inputs from the voltage regulation and reactive power regulation. Only the voltage regulation loop has been shown in Fig. 3(c). In addition, there are active damping terms given by,

$$\Delta \boldsymbol{v}_{dq} = \frac{sR_a}{s+\omega_b}\boldsymbol{i}_{dq}. \tag{3}$$

The active damping terms are subtracted from the voltage references to damp out oscillations in the IBESS output current. Finally, the current magnitude limiter is implemented to ensure that the IBESS current limits are not exceeded.

IV. Black Start of Onshore grid

Simulation studies are carried out to demonstrate the capability of the IBESS in providing black start service to the grid. It is a prerequisite that the OWPP operates in an islanded mode with the help of IBESS. This work is actually a continuation of the islanded operation of IBESS as described in the previous work [8]. Prior to initiating the black-start process, it is assumed that the OWPP is generating active power from 37 WTs with the power reference 0.15 pu on WT MVA base and deliver 0.064 pu (21 MW) due to 5% droop frequency response. After the losses are deducted, the remaining power is of the order of 13.8 MW at bus T2 and it is absorbed by the IBESS. This power depends upon the instantaneous operating condition of the OWPP. Additionally, it is considered here that the 220/400 kV onshore grid transformer is energized during the soft-charging of the system. It is essential that there is sufficient power and energy margin in the IBESS to perform the black start.

A. Test Cases and Success Criteria

The following test cases are envisaged:

- Energizing the onshore grid;
- Connection of block loads of 20 MW size.

The success criteria for the islanded operation was defined as follows:

- Steady-state frequency remains within the range of 47.5 – 52 Hz all the time;
- Voltage profile should be within the ±10% band around the nominal voltage;
- The IBESS current limits must not be violated.

B. Energizing Onshore Grid

The circuit breaker on the HV side of the grid transformer is closed at 30 s to energize the 400 kV OHL. The transformer voltage and currents on the HV side is shown in Fig. 4. The current waveform is far from sinusoidal. The rms values of the three-phase voltages and currents and the magnitudes of their harmonic components in the two cycles from 30.04 s to 30.06 s are shown in Table III for the first 5 harmonic orders. There is a rich 2nd harmonic component, amounting to 0.12, 0.12 and 0.13 pu in the three-phase current waveforms.

There is a first order filter of 20 ms time constant in the measurement of active and reactive power as well as the rms voltage. The oscillations in active power, reactive power and the rms voltage at the 220 kV bus T2, 400 kV bus T1 and the 33 kV load bus are shown in Fig. 5. Fourier analysis, for the 1st two cycles after 30 s, shows that the mean value of active power is 6.0 MW, and the mean reactive power is 18.9 Mvar in the first two cycles from 30 s to 30.04 s. Besides there is a lot of harmonic content, especially at the 2nd and the 4th harmonic orders. The three-phase voltage and the current waveform in the IBESS converter and the WT group (WTB1) are shown in Figs. 6 and 7.

Gradually, the oscillations decay and the reactive power flow into the onshore grid becomes capacitive as shown in Fig. 8. In due process the voltage in the offshore grid rises to 1.08 pu. At 42 s, 2.5 MW active power and $-j93.8$ Mvar reactive power flow to the grid. The three phase rms voltage

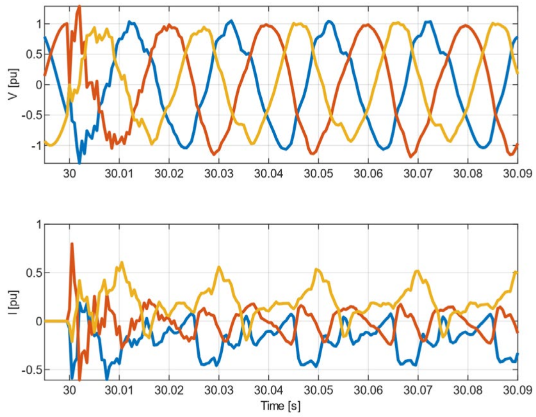

Fig. 4. Three phase voltage (top) and current (bottom) waveform on 400 kV terminals of the grid transformer during energization of OHL.

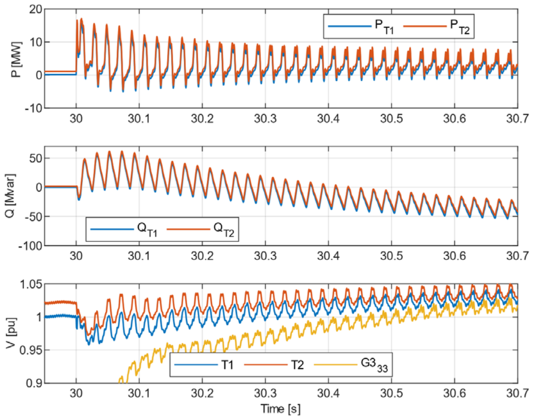

Fig. 5. Active power (top), reactive power (middle) and rms voltages (bottom) at different buses during energization of overhead line. T1, T2 and G33 indicate the corresponding bus names.

TABLE III. Voltages and currents Onshore grid transformer (Base 475 MVA, 400 kV rms, L-L).

	VA	VB	VC	IA	IB	IC
rms	0.99	1.04	0.95	0.34	0.17	0.36
mean	0.00	0.01	0.00	-0.19	-0.01	0.19
50 Hz	0.98	1.03	0.94	0.13	0.08	0.17
100 Hz	0.11	0.11	0.10	0.12	0.12	0.13
150 Hz	0.01	0.01	0.02	0.06	0.08	0.04
200 Hz	0.04	0.01	0.03	0.06	0.03	0.03
250 Hz	0.05	0.03	0.02	0.06	0.03	0.03

(computed by PSCAD) at different buses on the onshore grid is between 1.06 –1.08 pu as shown in Fig. 8.

C. Connection of block loads

The block loads are connected at 43 s, 45 s and 47 s, respectively, as shown in Fig. 8. Compared to the energization of the line, the block loads create negligible disturbance in the whole island grid. As the voltage at the load bus is higher than 1 pu, the actual supplied load is larger than the block size of 20 MW. The connected load is supplied initially by the IBESS as displayed in Fig. 9. As the output power of the IBESS increases, its frequency decreases. The WT units respond to the decreased frequency by ramping up their output power with a 5% droop response as shown in Fig. 10. This response from the WT helps to de-load the IBESS. The power flow at

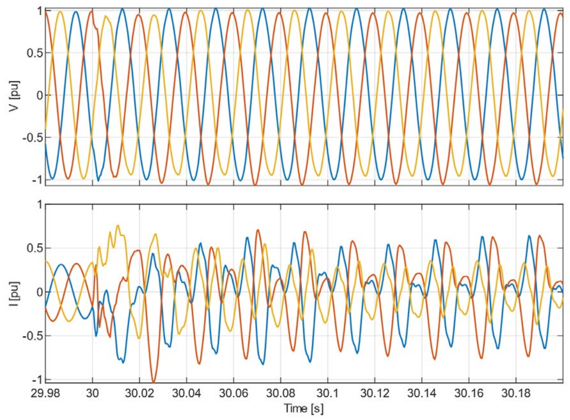

Fig. 6. IBESS converter terminal phase voltage (top) and current (bottom) waveforms during OHL energization.

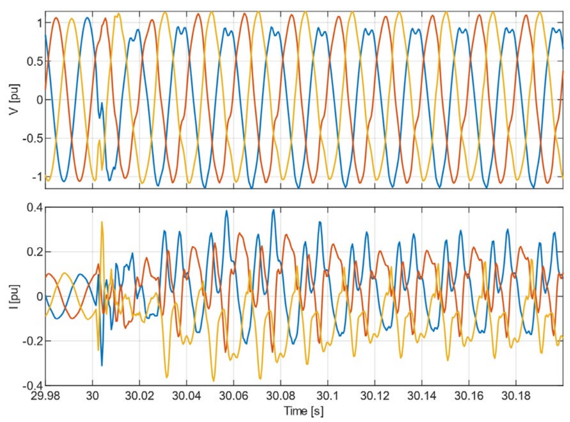

Fig. 7. WT group (WT6B1) converter terminal phase voltage (top) and current (bottom)waveforms during OHL energization.

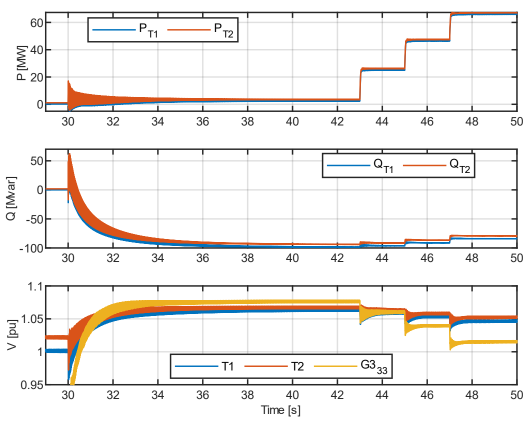

Fig. 8. Active power (top), reactive power (middle) and rms voltages (bottom) at different buses during OHL energization and block load connection. T1, T2 and G33 indicate the corresponding bus names.

the 220 kV bus T2, and the power of the IBESS corresponding to the block load connected at 33 kV are given Table IV.

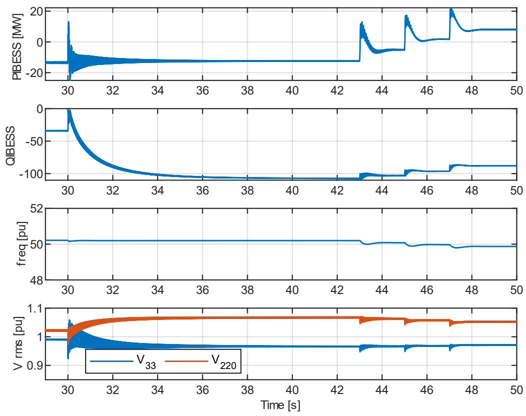

Fig. 9. Active power (top), reactive power (middle-top), frequency (middle-bottom) of the IBESS and rms voltages at the 33 kV and 220 kV terminals of IBESS transformer during OHL energization and connection of of block load.

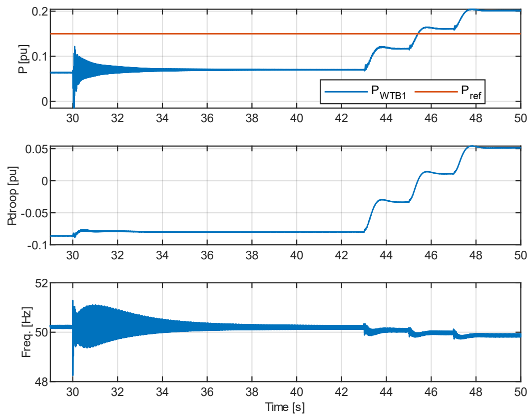

Fig. 10. WT group WTB: Active power reference, P_{ref}, and generated active power, P_{WTB1}, (top), droop power reference and PLL frequency during OHL energization and connection of of block load.

TABLE IV. POWERFLOW AND IBESS FREQUENCY CORRESPONDING TO CONNECTION OF 20 MW BLOCK LOADS.

		At T2 (220 kV)		Load at 33kV	IBESS	
Time [s]	**Load [MW]**	**P [MW]**	**Q [Mvar])**	**P [MW]**	**P [MW]**	**F [Hz]**
42.7	0	4	-94	0	-12.4	50.2
44.6	20	26.3	-91.6	22.5	-5.4	50.1
46.8	40	47.5	-86.5	43.2	1.9	50.0
48.8	60	67.0	-79.3	61.8	8.0	49.9

D. Overall Results

The success criteria for black start is fulfilled as the system maintains a stable voltage and frequency profile during the whole process. The voltages remain within 1.10 pu upper limit. The frequency remains well within the proposed limits of 47 to 52 Hz. In fact, the frequency deviation at the IBESS lies within ±0.2 Hz. This low value can be attributed to the 1.6% droop assigned to the IBESS. In the WT units the frequency is estimated by the phase locked loop (PLL), and it shows some oscillation during the transients produced by the switching of the OHL. Still, the frequency deviations at WT terminals is within ±1 Hz. These deviations do not affect the droop frequency response that is shown in Fig. 10, as the estimated frequency is filtered by a time constant of 0.5 s.

In the present work, the IBESS in grid forming control mode absorbs all the power imbalance in the grid. The WT responds only the to the resultant frequency deviations. There is a room for coordinating the loading of the IBESS and WT units.

V. CONCLUSIONS

This paper demonstrates the use of IBESS in the black start energization of the onshore grid. The IBESS converter in the grid forming control mode responds fast to the switching transients and sudden changes in active and reactive power flows during the closing of the long OHL as well as the grid connection of 20 MW block load units. While the closing of the long line produced large transients throughout the offshore grid including the IBESS controls, the block load connection appeared to be a relatively smooth event. The IBESS increased the output power to meet the increased demand and decreased the offshore grid frequency. Eventually, the WTs contributed the increased power demand as they responded to the decline in the offshore grid frequency.

REFERENCES

[1] A. Fernández-Guillamón, K. Das, N. A. Cutululis, and Á. Molina-García, “Offshore Wind Power Integration into Future Power Systems: Overview and Trends,” Journal of Marine Science and Engineering, vol. 7, no. 11, p. 399, Nov. 2019.

[2] PJM Manual 36: System Restoration, Rev. 28, June 22, 2020.

[3] National Grid ESO, ‘Black Start Strategy and Procurement Methodology 2020/2021’, 23 Jul. 2020.

[4] D. Pagnani, L. Kocewiak, J. Hjerrild, F. Blaabjerg, and C. L. Bak, “Overview of Black Start Provision by Offshore Wind Farms,” in Proceedings of IECON 2020, 2020.

[5] S. K. Chaudhary, X. Wang. D. Yang, R. Teodorescu, L. H. Kocewiak, M. P. S. Gryning, P. Johnson, C. Y. Chen, “Techno-economic Feasibility of a STATCOM with Battery Energy Storage for the Offshore Wind Power Plants,” in Proceedings of CIGRE Symposium Aalborg 2019, 2019.

[6] IBESS - Integrated Battery Energy Storage And Statcom for the Optimal Operation and Control of WPP in Power System, Aalborg University. Accessed on: Nov. 4, 2020. [Online]. Available: www.ibess.et.aau.dk.

[7] S. K. Chaudhary et al., “Challenges in Integration of MMC STATCOM with Battery Energy Storage for Wind Power Plants,” in Proceedings of 18th Wind Integration Workshop, 2019.

[8] S. K. Chaudhary et al., “Islanded Operation of Offshore Wind Power Plant using IBESS,” submitted to IEEE PES General Meeting, 2021.

[9] J. Hjerrild, S. Sahukari, M. Juamperez, Ł. H. Kocewiak, M. A. Vilhelmsen, J. Okholm, M. Zouraraki, T. Kvarts, “Hornsea Projects One and Two – Design and Execution of the Grid Connection for the World’s Largest Offshore Wind Farms”, Cigre Symposium Aalborg, Denmark, 4-7 June 2019.

[10] National Grid ESO, Black Start Technical Requirements. Accessed on 5 Nov., 2020. [Online] Available at https://www.nationalgrideso.com/black-start?technical-requirements.

[11] S. K. Chaudhary, A. F. Cupertino, R. Teodorescu, and J. R. Svensson, “Benchmarking of Modular Multilevel Converter Topologies for ES-STATCOM Realization,” Energies, vol. 13, no. 13, p. 3384, Jul. 2020.

[12] L. Zhang, L. Harnefors, and H.-P. Nee, “Power-Synchronization Control of Grid-Connected Voltage-Source Converters,” IEEE Trans.s on Power Systems, vol. 25, no. 2, pp. 809–820, May 2010.

[13] L. Harnefors, M. Hinkkanen, U. Riaz, F. M. M. Rahman, and L. Zhang, “Robust Analytic Design of Power-Synchronization Control,” IEEE Transactions on Industrial Electronics, vol. 66, no. 8, pp. 5810–5819, Aug. 2019.

.